



*Supplement of*

**Modular Multiplatform Compatible Air Measurement System (MoMuCAMS): a new modular platform for boundary layer aerosol and trace gas vertical measurements in extreme environments**

**Roman Pohorsky et al.**

*Correspondence to:* Roman Pohorsky ([roman.pohorsky@epfl.ch](mailto:roman.pohorsky@epfl.ch)) and Julia Schmale ([julia.schmale@epfl.ch](mailto:julia.schmale@epfl.ch))

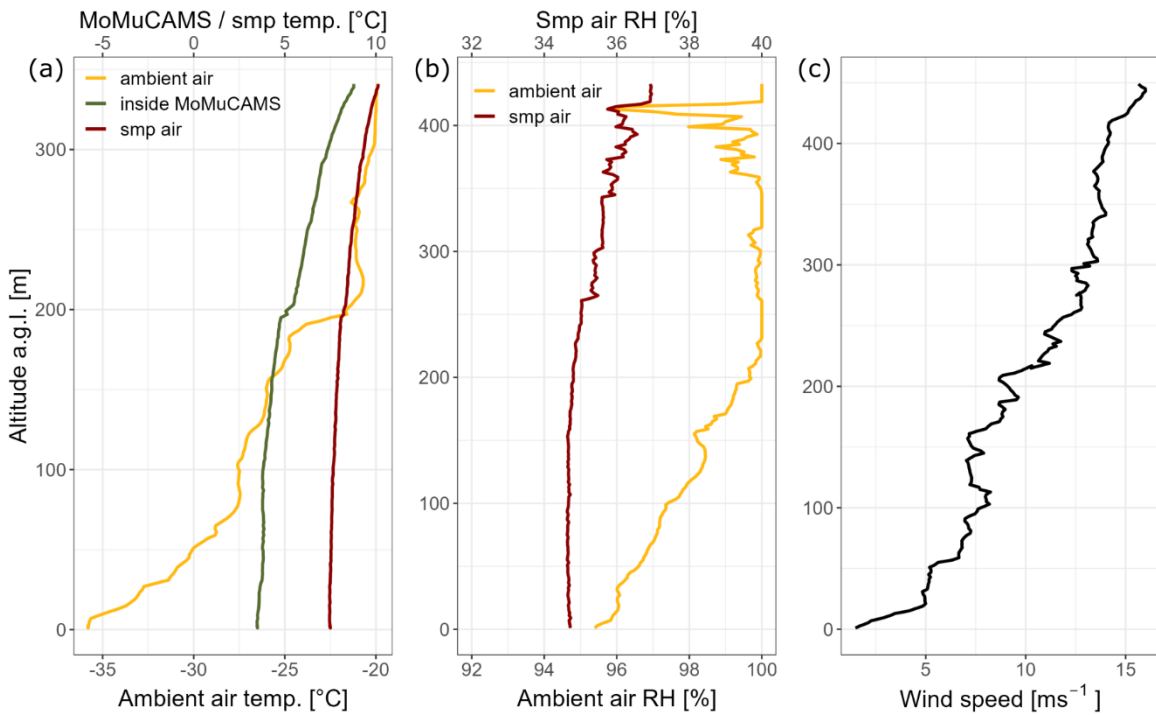
The copyright of individual parts of the supplement might differ from the article licence.

## S.1 MoMuCAMS and helikite performance

5

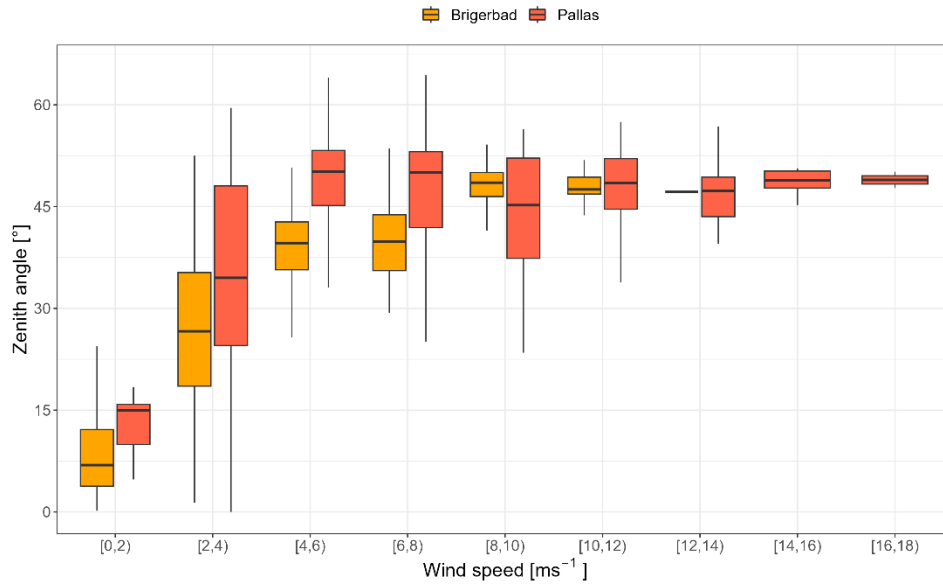


10 **Figure S1: MoMuCAMS with the additional radiation shielding for temperature sensors installed on the side (in the red ellipse). The tube shaped radiation shield includes a net on the front to prevent condensation of water directly on the sensors and a fan in the back to provide active flow of air through the tube. Two T and RH sensors (SHT85, Sensirion, CH) are placed in the middle of the tube.**



15

**Figure S2: Vertical profiles of (a) Ambient, sampled and MoMuCAMS internal air temperature, (b) ambient and sampled relative humidity and (c) wind speed. Profile (a) was measured in Fairbanks, USA (64°51'12" N / 147°51'34" W) on January 30, 2022. Profiles (b) and (c) were measured in Pallas, Finland (68°00'00" N / 24°14'22" E) on October 8 and October 13, 2022, respectively.**



20

**Figure S3: Box plots of the helikite's tether zenith angle against measured wind speed. The zenith angle was estimated from the horizontal displacement given by recorded GPS location during flight and the calculated barometric altitude. Colors are indicative of two field campaigns. Orange corresponds to Brigerbad (46°18'00" N / 7°55'16" E), in a Swiss alpine valley, and red corresponds to Pallas in Finland (68°00'00" N / 24°14'22" E).**

25

S.2 aMCPC cross-comparison and  $d_{50}$  cutoff characterization

30

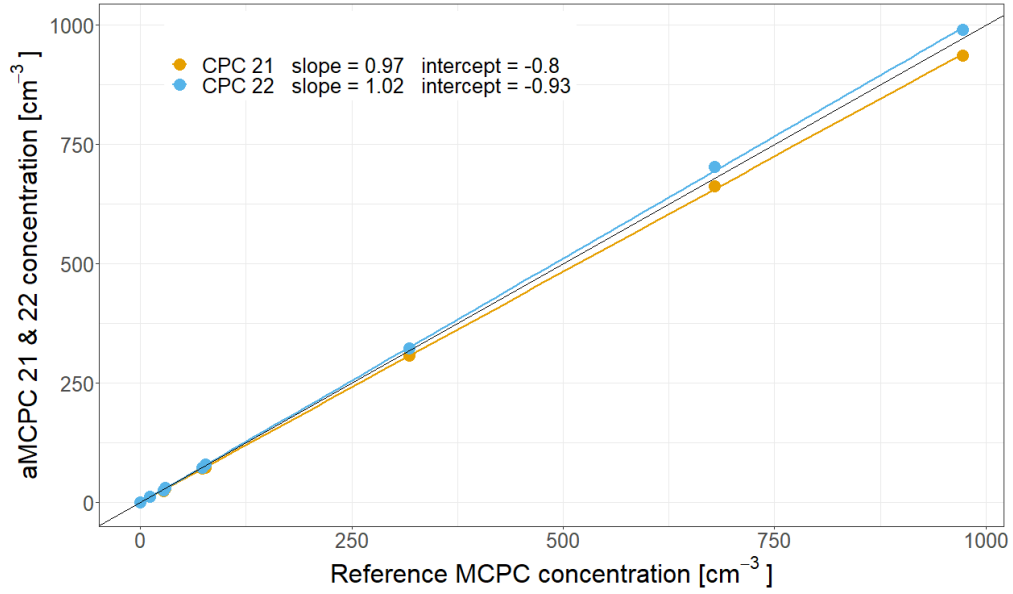


Figure S4: Comparison of two aMCPCs (model 9403, Brechtel Manufacturing Inc) against a reference MCPC (model 1720, Brechtel Manufacturing Inc).

35

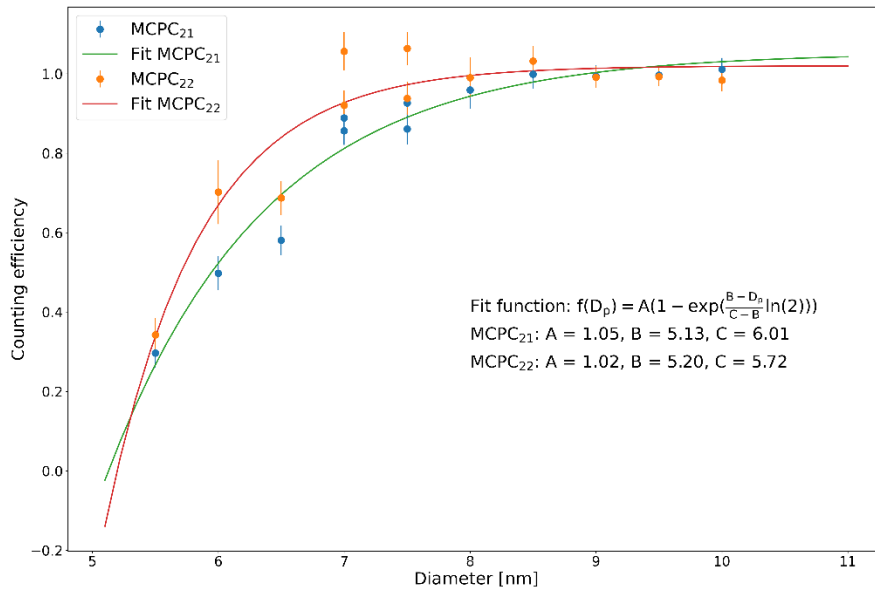
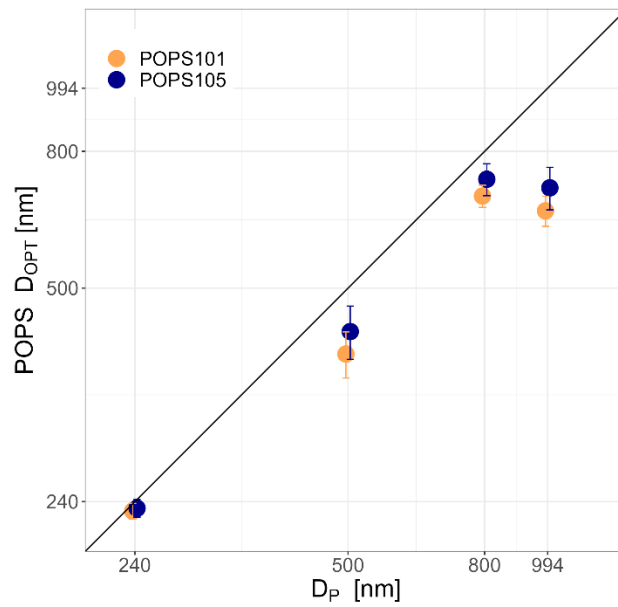


Figure S5. Counting efficiency for aMCPC 21 and 22. The fitting function indicates a  $d_{50}$  cutoff of 6 nm for aMCPC 21 and 5.7 nm for aMCPC 22.

40

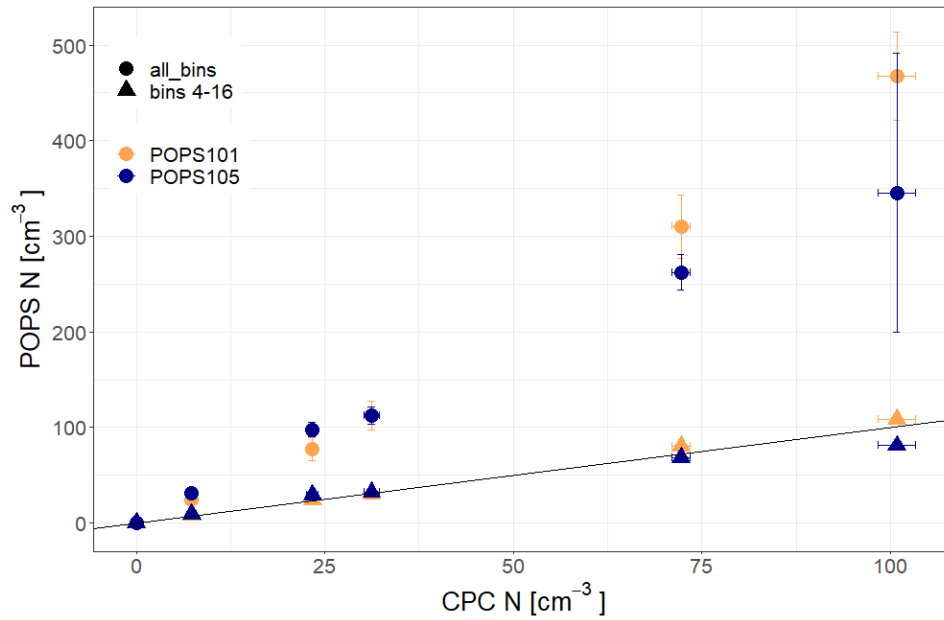
45

### S.3 POPS (Printed Optical Particle Spectrometer) Sizing and counting efficiency characterization details



50

Figure S6. Measured optical particle diameter ( $D_{OPT}$ ) by two POPS determined by lognormal fits of the measured particle size distribution (PSD) of PSL particles with a given mobility diameter ( $D_P$ ). The black line represents the 1:1 line.

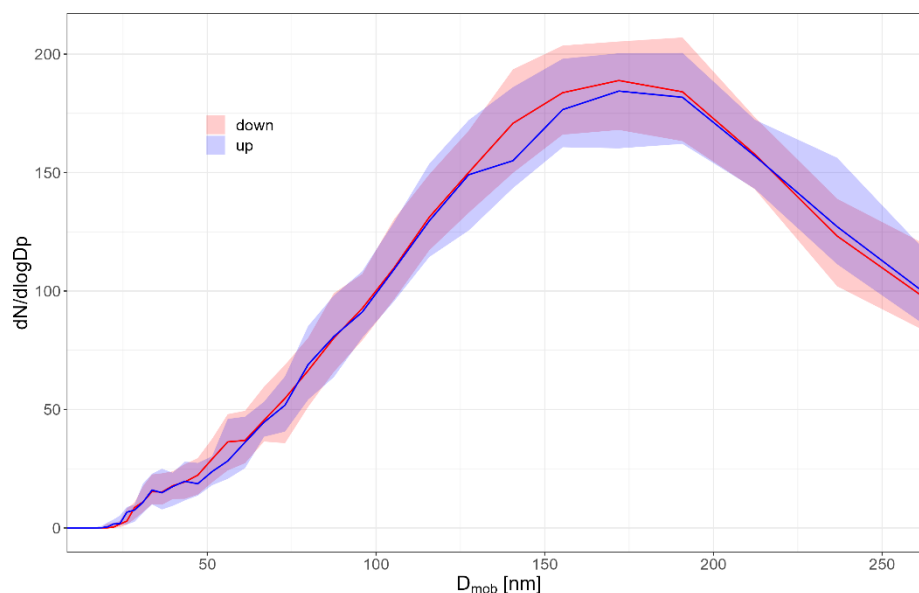


55

Figure S7. Particle number concentration of two POPS against a reference CPC. Dots represent mean concentration including all bins and triangles represent recalculated mean concentrations excluding bins 1 to 3.

60

## S.4 mSEMS performance evaluation



65 **Figure S8: 6-hour comparison of “up” versus “down” scans with the mSEMS. Full line indicates the median PNSD. Shadings represent the interquartile range.**

**Table S1: Comparison of particle counting for different size ranges between the mSEMS and the SEMS.**

	8 to 15 nm	15 to 30 nm	30 to 50 nm	100 to 150 nm	150 to 250 nm
$N_{mSEMS} / N_{SEMS}$	1.40	1.36	0.97	0.96	1.05

70

## S.5 Element analysis for collected aerosols with the HFI

Before sampling, all filters are baked for 6 hours at 550° C in separate aluminium pouches to reduce contaminants in the blanks and directly sealed in plastic zip-bags. We collect regular blanks for each sampling campaign. In particular, we have two types of campaign blanks: regular blanks and field blanks. The former are brought to the field but not taken out from their aluminium pouches (regular blank). The latter are installed in the filter sampler and retrieved shortly after to mimic field operations (field blank). After sampling, loaded filters are retrieved, folded in half and placed back in their respective pouches. Retrieval of filters is performed, if possible, at temperature conditions similar to sampling conditions to avoid any evaporation of volatile compounds.

80 Filters are then stored at -20° C before analysis.

### S.5.1 Microwave assisted digestion of aerosol filters

85 For each regular filter blank, field blank and aerosol sample, half of the filter was cut with stainless steel scissors and placed into a polytetrafluoroethylene (PTFE) microwave vessel. 1 mL of nitric acid (69% HNO<sub>3</sub>, Suprapur; Roth) 1 mL of hydrogen peroxide (30% H<sub>2</sub>O<sub>2</sub>, for ultratrace analysis; Sigma-Aldrich), and 1 mL of ultrapure water (18.2 MΩ cm; Nanopure DIAMOND™ system) were then added to the PTFE microwave vessel. The digestion was performed immediately with an MLS GmbH UltraCLAVE 4 microwave using the following program: temperature ramp from 25 to 230°C over 25 min (Power, 2500W; P, 130 Bar) and then,

90 20 min at 230°C (Power, 2500W; P, 130 Bar). After digestion, the 6 mL sample digests were poured into 15 mL polypropylene vials, and 3 mL of ultrapure water was used to recover the remaining sample digest in the digestion vessel, which was then added to the 6 mL sample digest. The digests were then filtered at 0.45 µm (syringe filter Perfect-Flow®, Nylonmembran; BGB Analytix) and stored in the dark at 4°C until analysis. In addition to regular filter blank and field blanks, 3 procedural blanks, i.e., reagent blanks that consist of the digestion reagents subjected to the same digestion, filtration and storage procedures as the samples and filter blanks were performed. To ensure low element background in the digest, the PTFE microwave vessels were extensively cleaned before digestion of the regular filter blanks, field blanks and aerosol samples. The PTFE microwave vessels cleaning consisted of: 1) soaking them in 20 % HNO<sub>3</sub> (from 69% HNO<sub>3</sub>, ISO; Roth) overnight; 2) rinsing them three time with ultrapure water; 3) soaking them in 20% HCl (from 35% HCl, ISO; Roth) overnight; 4) rinsing them three time with ultrapure water; 5) soaking them in 20 % HNO<sub>3</sub> (from 69% HNO<sub>3</sub>, ISO; Roth) overnight; 6) rinsing them three time with ultrapure water; and 7) performing a digestion run with the vessels filled up with 3 mL of ultrapure water and 3 mL of HNO<sub>3</sub> (69%, Suprapur; Roth) using the same microwave program than for the sample digestion.

95 The resulting detection limits are calculated according to IUPAC recommendation (McNaught and Wilkinson, 1997), i.e., the mean plus three times the standard deviation of obtained blank concentrations. The background levels obtained for other trace elements and resulting detection limits are presented Table S2. Results of regular and field blanks revealed no difference in the levels of trace elements, suggesting that the substrate itself and the digestion step are the largest sources of contaminations.

100 **Table S2: Background levels of blank filters and detection limits of analyzed elements**

Element	Unit	Mean of background	Standard deviation of background	Detection limit
Aluminum (Al)		4	4	16
Calcium (Ca)		0.16	0.09	0.43
Chromium (Cr)		0.08	0.03	0.16
Iron (Fe)		1.2	0.2	1.9
Magnesium (Mg)		0.24	0.06	0.43
Nickel (Ni)	µg	0.08	0.02	0.15
Phosphorus (P)		0.18	0.07	0.39
Potassium (K)		0.05	0.03	0.15
Sodium (Na)		0.18	0.09	0.43
Sulfur (S)		1.1	0.3	2.0
Zinc (Zn)		0.8	0.3	1.8
Arsenic (As)		0.7	0.2	1.3
Cadmium (Cd)		0.4	0.3	1.3
Cobalt (Co)		0.9	0.4	2.0
Copper (Cu)		8	5	22
Lead (Pb)		9	4	22
Manganese (Mn)	ng	16	5	30
Molybdenum (Mo)		17	3	25
Rubidium (Rb)		0.8	0.8	3.2
Selenium (Se)		0.05	0.02	0.12
Silver (Ag)		0.12	0.06	0.30
Vanadium (V)		0.9	0.7	3.1

## S.5.2 Quantification of elements by ICP-MS/MS

Elements were quantified in the digests using an Agilent 8900 ICP-MS/MS equipped with an SPS4 autosampler, a high-throughput injection system (ISIS) with a PTFE sample loop, a concentric nebulizer, a Scott double-pass spray chamber cooled to 2°C, a 2.5 mm i.d. quartz torch, and platinum sampler and skimmer cones. All ICP-MS/MS parameters were optimized before analysis using a tuning solution containing 10 µg L<sup>-1</sup> of lithium (Li), yttrium (Y), cobalt (Co), cerium (Ce), and tellurium (Te) (prepared with standards from J.T. Baker). Employed acquisition parameters, i.e., collision/reaction cell gas(es), single versus tandem MS mode, acquired mass to charge ratio (*m/z*), acquisition time and number of analytical replicates are given for each analyzed elements in Table S3. Quantification was done by external calibration with elemental standards (purchased at J.T. Baker) prepared in the sample digest matrix (i.e., 11% HNO<sub>3</sub> Suprapur). An internal standard containing scandium (Sc, 70 µg L<sup>-1</sup>), indium (In, 7 µg L<sup>-1</sup>) and lutetium (Lu, 7 µg L<sup>-1</sup>) was used during the analysis to check signal stability during the runs. ICP-MS/MS data-treatment was done using Agilent Masshunter software (version 4.6).

**Table S3:** ICP-MS/MS acquisition parameters for analyzed elements

Elements	ICP-MS/MS mode	Acquired <i>m/z</i>	Acquisition time (s)	Replicates number
Sodium (Na)		23	0.01	
Magnesium (Mg)		24	0.01	
Aluminum (Al)		27	0.01	
Potassium (K)	Single quadrupole mode –	39	0.01	3
Calcium (Ca)	C/RC: 5 mL min <sup>-1</sup> He	43	0.01	
Vanadium (V)		51	0.1	
Iron (Fe)		56	0.05	
Zinc (Zn)		66	0.1	
Chromium (Cr)		52->52	0.1	
Manganese (Mn)		55->55	0.1	
Cobalt (Co)		59->59	0.1	
Nickel (Ni)		60->60	0.1	
Copper (Cu)		63->63	0.1	
Arsenic (As)	Tandem MS mode –	75->75	0.3	3
Selenium (Se)	C/RC: 5 mL min <sup>-1</sup> H <sub>2</sub>	78->78	0.3	
Rubidium (Rb)		85->85	0.1	
Molybdenum (Mo)		98->98	0.1	
Silver (Ag)		107->107	0.1	
Cadmium (Cd)		111->111	0.1	
Lead (Pb)		208->208	0.1	
Phosphorus (P)	Tandem MS mode –	31->47	0.05	3
Sulfur (S)	C/RC: 30% O <sub>2</sub> + 1 mL min <sup>-1</sup> H <sub>2</sub>	32->48	0.05	

## S.6 Electron microscopy

### S.6.1 Scanning electron microscopy with energy dispersive x-ray analysis (SEM/EDX)

For scanning electron microscopy, the analysis is carried out on a Thermo-Scientific Teneo. This machine is equipped with a Bruker XFlash EDX detector, as well as Everhart-Thornley and Trinity (in-column) electron detectors. Imaging and EDX spectroscopy are performed using a beam energy of 5 keV. A focused electron probe is scanned over a region of interest to collect EDX data in the form of spectrum images. For each region of interest, a second EDX map using a beam energy of 15 kV is acquired in case of ambiguity or peaks that overlap. To account for the signal from the sampling substrate, the beam is first focused on an aerosol free substrate area (red trace in Fig. S8). Before analysis, filters are coated with a 7-nm iridium layer to avoid charge accumulation at their surface. Two examples of particles collected during airborne filter sampling on September 28 and October 7, 2021 are shown on Fig. Figure S8. EDX spectra for particle (a) shows traces of N, O, Fe and Si. Particle (b) shows traces of N,



Si, Al and K. Details on sample collection are presented in Sect. 4.3; however, a full analysis of SEM/EDX results is beyond the scope of this paper, which serves mainly as proof of concept for airborne aerosol sampling and subsequent microscopy analysis.

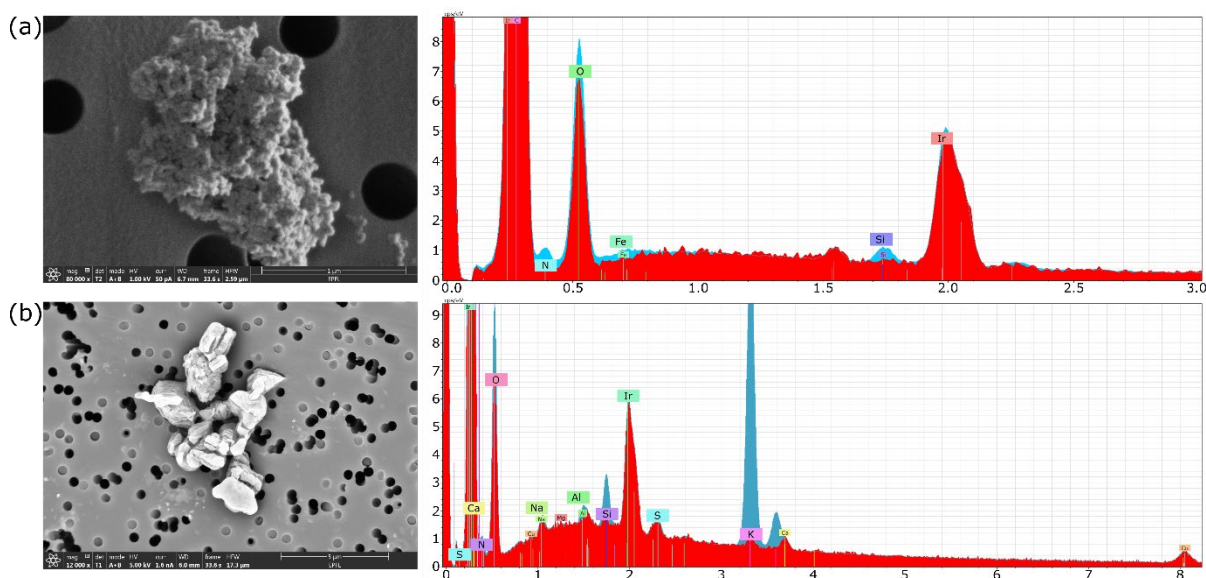
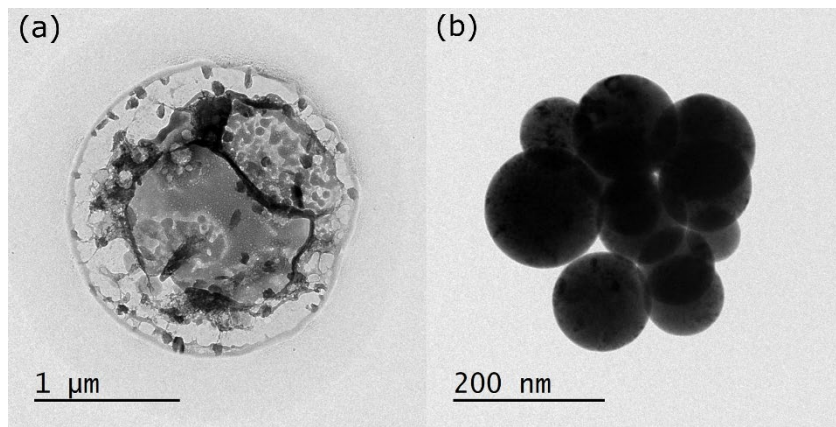


**Figure S9: SEM/EDX of two particles collected during airborne sampling on a) September 28 and b) October 7, 2021. Red spectra represent the EDX signal collected when pointing the electron beam only on the filter substrate which serves as a type of blank. Blue spectra indicate the EDX signal from the particle. (The SEM pictures were obtained in collaboration with Emad Oveisi, EPFL)**

### S.6.2 Transmission electron microscopy (TEM)

For transmission electron microscopy, the analysis is performed on a Thermo Scientific Tecnai Spirit operating at an accelerating voltage of 120 kV. The images are acquired under bright field imaging conditions, in which only the directly transmitted beam, selected by the objective aperture, contributes to the image formation. TEM was performed on collected samples and confirmed that the system could effectively collect aerosol particles for TEM observations. An example of two particles collected during the September 28 flight is shown in Fig. S9. Particle (a) presents a heterogeneous composition of an internally mixed particle with a denser core surrounded by lighter elements, as indicated by the brighter shading and a spherical shape. Particle (b) is an agglomerate of more homogeneous particles, likely composed of soot. Similarly to the SEM/EDX example, these results are mainly presented for illustrative purposes of the system's capabilities for aerosol sampling and analysis and a more detailed interpretation is beyond the scope of this paper.



165 **Figure S10: TEM images of two particles collected during airborne sampling on September 28. The images are acquired under bright field imaging conditions at an accelerating voltage of 120 kV. (The TEM pictures were obtained in collaboration with Emad Oveisi, EPFL)**

170

175

180

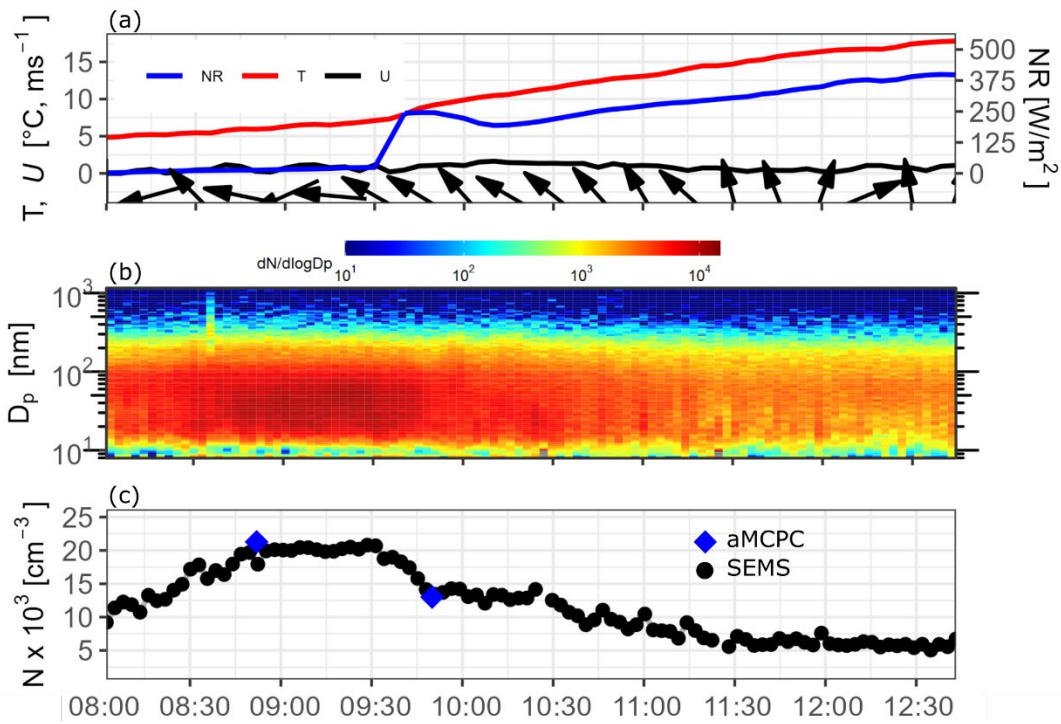
185

190

S.7 Field application

195

S.7.1 Case 1 – Evolution of aerosol and trace gas concentrations during a surface inversion dissipation



200

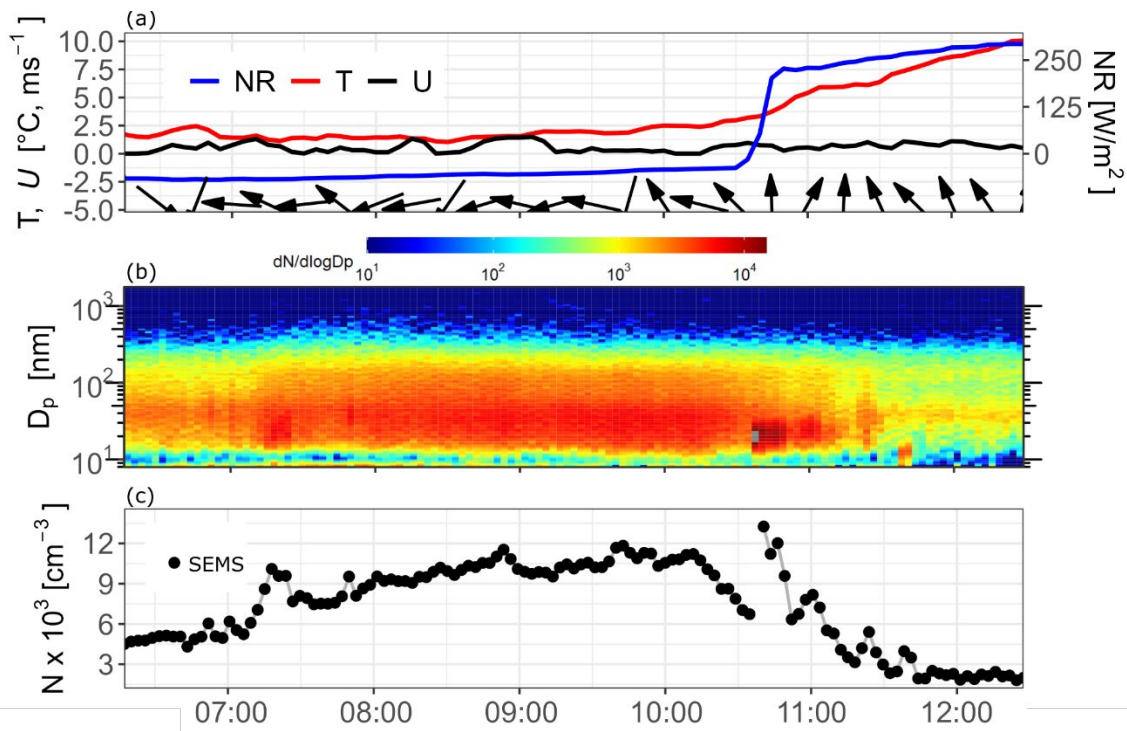
Figure S11: Time-series on October 1, 2022 of (a) temperature (T), net radiation (NR) and wind speed (U) and direction (arrows) measured at the surface, (b) measured particle size distribution at the surface and (c) integrated total concentration (black dots) at the surface. Blue diamonds indicate the measured particle concentration (N<sub>7</sub>) onboard MoMuCAMS when the helikite was at the surface.

205

210

215

S.7.2 Case 2 – Particle size distribution dynamics during the transition from a stable to a mixed boundary layer



220

Figure S12: Timeseries on October 14, 2022 of (a) temperature (T), net radiation (NR) and wind speed (U) and direction (arrows) measured at the surface, (b) measured particle size distribution at the surface and (c) integrated total concentration at the surface.